PCCP

Accepted Manuscript

ROYAL SOCIETY OF CHEMISTRY

www.rsc.org/pccp

Assessing the Performance of MM/PBSA and MM/GBSA Methods. 4. Accuracies of MM/PBSA and MM/GBSA Methodologies Evaluated by Various Simulation Protocols using PDBbind Data Set

Huiyong Sun[a,b], Youyong Li[a], Sheng Tian[a], Lei Xu[b], Tingjun Hou[a,b*]

[a]Institute of Functional Nano & Soft Materials (FUNSOM) and Collaborative Innovation Center of Suzhou Nano Science and Technology, Soochow University, Suzhou, Jiangsu 215123, China.

[b]College of Pharmaceutical Sciences, Zhejiang University, Hangzhou, Zhejiang 310058, China

Running Title: Accuracies of MM/PBSA and MM/GBSA evaluated by a large dataset

Corresponding author:

Tingjun Hou

E-mail: tingjunhou@zju.edu.cn or tingjunhou@hotmail.com

Phone: +86-512-65882039

Keywords: MM/GBSA, MM/PBSA, Generalized Born, Poisson Boltzmann, Binding free energy, PDBbind

For Table of Contents Use Only

Formal Charges

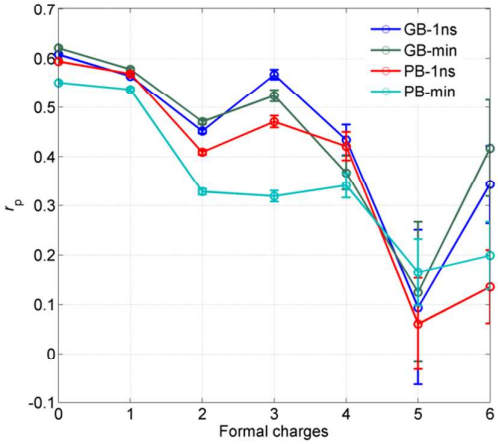

Fold Family

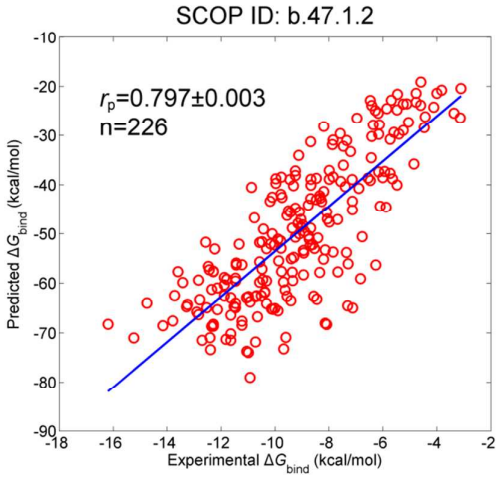

Abstract

By using different evaluation strategies, we systemically evaluated the performance of Molecular Mechanics/Generalized Born Surface Area (MM/GBSA) and Molecular Mechanics/Poisson-Boltzmann Surface Area (MM/PBSA) methodologies based on more than 1800 protein-ligand crystal structures in the PDBbind database. The results can be summarized as follows: (1) for the one-protein-family/one-binding-ligand case which represents the unbiased protein-ligand complex sampling, both MM/GBSA and MM/PBSA methodologies achieve approximately equal accuracies at the interior dielectric constant of 4 (with r_p=0.408±0.006 of MM/GBSA and r_p=0.388±0.006 of MM/PBSA based on the minimized structures); while for the total dataset (1864 crystal structures), the overall best Pearson correlation coefficient (r_p=0.579±0.002) based on MM/GBSA is better than that of MM/PBSA (r_p=0.491±0.003), indicating that biased sampling may significantly affect the accuracy of the predicted result (some protein families contain too many instances and can bias the overall predicted accuracy). Therefore, family based classification is needed to evaluate the two methodologies; (2) the prediction accuracies of MM/GBSA and MM/PBSA for different protein families are quite different with r_p ranged from 0 to 0.9, whereas the correlation and ranking scores (an averaged r_p/r_s over a list of protein folds and also representing the unbiased sampling) given by MM/PBSA (r_p-score=0.506±0.050 and r_s-score=0.481±0.052) are comparable to those given by MM/GBSA (r_p-score=0.516±0.047 and r_s-score=0.463±0.047) at the fold family level; (3) for the overall prediction accuracies, molecular dynamics (MD) simulation may not be quite necessary for MM/GBSA ($r_{p\text{-minimized}}$=0.579±0.002 and $r_{p\text{-1ns}}$=0.564±0.002), but is needed for MM/PBSA ($r_{p\text{-minimized}}$=0.412±0.003 and $r_{p\text{-1ns}}$=0.491±0.003). However, it depends when facing up with individual systems; (4) both MM/GBSA and MM/PBSA may be unable to give successful predictions for the ligands with high formal charges, with the Pearson correlation coefficient ranged from 0.621±0.003 (neutral ligands) to 0.125±0.142 (ligands with 5 formal charges). Therefore, it can be summarized that,

although MM/GBSA and MM/PBSA perform similarly in the unbiased dataset, for the currently available crystal structures in PDBbind database, compared with MM/GBSA, which may be used in multi-targets comparison, MM/PBSA is more sensitive to the investigated systems, and may be more suitable for individual-target-level binding free energy ranking. This study may provide useful guidance for the post-processing of docking based studies.

Introduction

The MM/GBSA and MM/PBSA approaches have been widely used in free energy calculations.[1-27] Compared with the theoretically rigorous methods such as free energy perturbation (FEP) and thermodynamic integration (TI),[28-30] MM/GBSA and MM/PBSA are more computationally efficient and convenient with few rules having to be obeyed, such as various constrain rules in FEP/TI.[31-34] For the MM/GBSA and MM/PBSA calculations, the separate trajectory strategy, namely using the trajectories of complex, receptor, and ligand separately, is more theoretically rigorous due to the consideration of the conformational change of the receptor and ligand when a free ligand binds to an unbound-state receptor.[2, 35, 36] However, the intramolecular energies, such as bond energy, angle energy, etc., cannot be well canceled, and consequently leading to a large uncertainty or noise of the predicted binding free energies.[36] On the contrary, the binding free energy predicted by a single trajectory (a trajectory containing only ligand-receptor complex) is more stable and this strategy has been widely used in previous studies.[27, 37-40] The binding free energy can be calculated by MM/PBSA or MM/GBSA according to the following equations:

$$\Delta G_{bind} = G_{com} - (G_{rec} + G_{lig}) \quad (1)$$

$$\Delta G_{bind} = \Delta H - T\Delta S \approx \Delta E_{MM} + \Delta G_{sol} - T\Delta S \quad (2)$$

$$\Delta E_{MM} = \Delta E_{internal} + \Delta E_{electrostatic} + \Delta E_{vdw} \quad (3)$$

$$\Delta G_{sol} = \Delta G_{PB/GB} + \Delta G_{SA} \quad (4)$$

where ΔG_{bind} denotes the binding free energy and it can be decomposed into three terms: (1) the molecular mechanical energy (ΔE_{MM}), which is the summation of the intramolecular energy ($\Delta E_{\text{internal}}$, including bond, angle, and dihedral energies), electrostatic energy ($\Delta E_{\text{electrostatic}}$), and van der Waals energy (ΔE_{vdw}) (Equation 3); (2) the solvation energy (ΔG_{sol}), which is composed of the polar ($\Delta G_{\text{PB/GB}}$) and non-polar contributions (ΔG_{SA}) (Equation 4); and (3) the entropic contribution (-TΔS), which is associated with the conformational entropy loss when a free-state ligand binds to the corresponding unbound-state receptor. Although the solvation energy calculated by Poisson-Boltzmann (PB) equation is thought to be more accurate than that solved by generalized Born (GB) models due to the reason that it is more physically sound, the rapidly developed GB models[41-45] may be more competent in accurately calculating the solvation energy, such as the GB model developed by Onufriev (GB^{OBC1}) was found more accurate than the PB model embedded in Delphi II in our previous study.[46] Therefore, to give a comprehensive comparison, both the PB and GB approaches were used for the solvation energy calculations in this study.

Various guidelines and protocols have been proposed by previous studies for the MM/PBSA and MM/GBSA calculations.[46-52] For instance, Genheden and coworkers have evaluated the different protocols for the calculation of entropy and declared that it is reasonable to use a truncated model to calculate the conformational entropy.[47] Maffucci et al. have studied how water molecules affect the prediction for ligand binding and found that when an explicit ligand hydration shells with 30~70 water molecules around the ligand was used, the MM/GBSA prediction could be significantly improved.[49] Weis and colleagues have examined the impact of different force fields, solvent models, and boundary conditions to the avidin system bounded with seven biotin analogues, and shown that the MM/GBSA predictions based on different force fields and boundary conditions do not have large difference, but explicit water model is necessary.[50] Greenidge et al. computed the binding free energies to a set of crystal structures in the PDBbind database (855 crystal structures)

by using the MM/GBSA approach based on a variable dielectric GB model,[53] and the predicted binding free energies show good correlation with the experimental data (the Pearson correlation coefficient is ~0.79).[52] However, as analyzed in this study, it may need to use a larger dataset to give more reliable and comprehensive evaluation for MM/PBSA and MM/GBSA. Our group has also hierarchically studied the influences of different GB and PB models, length of simulation time, entropy effects, solute dielectric constants, force fields, and ligand charge models on the prediction accuracies of MM/GBSA and MM/PBSA.[46, 48, 51] However, all the studies discussed above have focused on certain systems (at most 6 or 7 systems), and the results may be biased from the evaluation of the overall accuracies of MM/GBSA and MM/PBSA. Therefore, in this study, based on the well-tested strategy from our previous studies,[46, 48, 51] we have systemically evaluated the overall accuracies of the MM/GBSA and MM/PBSA methodologies based on more than 1800 protein-ligand complexes derived from the PDBbind database.[54, 55]

Materials and Methods

Preparation of the Dataset and Initial Simulation Structures

1872 no-metal containing complexes in the protein-ligand refined set were downloaded from the PDBbind database (version 2011) and 1864 were used for the evaluation,[54-56] where each complex has a K_i or K_d value (the detailed information can be found in Supporting Information Table S1). The experimental free energy (ΔG_{bind}) was estimated by Equation (5), where T was set to 298 K. Although numerous studies have emphasized the way of choosing accurate experimental data to get more reliable results,[52, 57] we did not employ predefined rules to select a sub-database to do the calculations due to the reason that no matter how accurate the experimental data is, uncertainty of errors still exists, and the common experimental results (without using extremely strict experimental methods) should be reasonable for the evaluation of currently widely used methods.[57] Nevertheless, the purpose of this study is to evaluate the overall accuracies of the MM/GBSA (GB^{OBC1}) and MM/PBSA (PB^{pbsa})

methodologies, rather than optimizing these methods.

$$\Delta G_{bind} = -RT \ln \frac{1}{K_i} \quad \text{or} \quad \Delta G_{bind} = -RT \ln \frac{1}{K_d} \qquad (5)$$

To automatically process the ligand-receptor complexes, the *tleap* and *antechamber* modules in AMBER11 were used to construct the topology files for the investigated proteins and ligands, namely, all the protonation states and the ligand charges were determined by the default parameters in AMBER11,[58] such as the residues of HIS were all parameterized to HIE. Since the AM1-BCC (AM1 with bond charge corrections) charges[59] performed well in our previous work,[51] the partial charges for each ligand were fitted using the AM1-BCC method embedded in the *sqm* program in AMBER11.[60] Counterions of Na^+ or Cl^- were added where has the lowest or highest electrostatic potential to neutralize the systems. The ff03 force field[61] was employed for the proteins because it performed well in short-time MD simulation as evaluated by our previous work.[51] The General Amber force field (gaff) was used for the ligands.[62] Each system was immersed in a TIP3P water box[63] with the water molecules extended 10 Å of the solute in each direction.

Molecular Dynamics (MD) simulations

Before MD simulations, each system was minimized using a protocol with three steps: at first, all the backbone heavy atoms of the protein were constrained with an elastic constant of 50 kcal/mol·Å^2 and the other atoms were free (500 cycles of steepest descent and 500 cycles of conjugate gradient minimization); next, the elastic constant was weakened to 10 kcal/mol·Å^2 (500 cycles of steepest descent and 500 cycles of conjugate gradient minimization); at last, the whole system was set free and minimized for 5000 steps (1000 cycles of steepest descent and 4000 cycles of conjugate gradient minimization). The Particle mesh Ewald (PME) algorithm was employed to handle the long-range electrostatics.[64] All the covalent bonds involving hydrogen atoms were constrained using the SHAKE algorithm,[65] and the time step was set to 2 fs. Each system was gradually heated from 0 to 300 K in the NVT ensemble over a period of 50 ps, and then relaxed by 50 ps in the NPT ensemble with

the temperature and pressure maintained at 300 K and 1 atm. Finally, 1 ns production simulations were performed for each system. The snapshots were collected at an interval of 5 ps, namely, 200 frames for each system.

Free energy calculations

The MM/GBSA and MM/PBSA approaches were employed for the evaluation of the binding free energy. For the solvation term of the free energy, according to our previous work,[46] the modified GB model developed by Onufriev[41] (GB^{OBC1}) performed better than the other two GB models (GB^{OBC2} and GB^{HCT}) and the PB model embedded in Delphi II program.[66] Thus, in this study, the GB^{OBC1} model was used for the calculation of the solvation energy. Moreover, recently we found that the PB model developed by Tan and Luo (noted as PB^{pbsa} in Amber11)[67] could give better predictions to some systems compared with the GB^{OBC1} model.[51] Therefore, the PB model developed by Tan and Luo was also employed to make an evaluation. The exterior dielectric constant (dielectric in bulk) was set to 80, and the interior dielectric constant (dielectric in solute) was set to 1, 2 or 4 as we did previously to give a comparison. No ionic strength was added to the MM/GBSA or MM/PBSA calculations. Due to the expensive computational demand and no apparent improvement of the predictions,[37, 47, 48, 68] the entropy term was not included in the binding free energy calculation. Therefore, the free energy calculated here, in fact, is enthalpy or say that effective binding free energy. The non-polar part of the solvation energy (ΔG_{SA}) was estimated by the LCPO algorithm based on the solvent accessible surface area (SASA, ΔA).[69] The parameters are illustrated in Equation (6), where γ and b were set to 0.0072 and 0, respectively. For each system, the binding free energy was calculated using both the 1 ns MD trajectory (based on 200 frames) and the minimized structure (the final-optimized frame after the three stages of minimization as mentioned above) to give a comparison.

$$\Delta G_{SA} = \gamma \Delta A + b \qquad (6)$$

Estimation methods. The Pearson correlation coefficient (r_p) and Spearman ranking coefficient (r_s) in conjunction with random sampling were used for the estimation of the linear correlation and ranking power of the predictions (all the uncertainties were reported in standard error). Although the Spearman ranking coefficient is useful in the ranking of the binding free energies,[48, 51] The Pearson correlation coefficient is more appropriate when a large dataset is to be evaluated. Therefore, the analyses will be more focused on the Pearson correlation coefficient.

In order to give a more detailed landscape of the two methodologies, proteins should be divided into clusters. Unfortunately, it will be hard for the multiple sequence alignment algorithm (MSA)[70] to cluster a large dataset using pairwise-based sequence similarity method. Thanks to the establishment of *Structural Classification of Proteins* database (SCOP) that used a structural similarity-based algorithm to classify proteins into different scaffolds,[71, 72] 1546 out of 1864 tested proteins were successfully assigned to 240 different protein fold families according to the indexes of the SCOP database (version 1.75B).

Results and Discussion

The overall prediction accuracies of MM/GBSA and MM/PBSA

As shown in Table I, the overall accuracy of MM/GBSA is better than that of MM/PBSA based on not only the minimized structures, but also the 1 ns MD trajectories calculated by 1, 2 or 4 inner dielectric constant. Interestingly, the MM/GBSA calculations based on the minimized structures with the inner dielectric constant of 4 achieve the best accuracy with the Pearson (r_p) and Spearman (r_s) coefficients up to 0.579 and 0.602, respectively (Figure 1), and they are slightly better than the MM/GBSA calculations based on the MD trajectories (r_p=0.564±0.002 and r_s=0.591±0.002). The reason why the prediction accuracy of MM/GBSA based on the 1 ns MD trajectories is a bit worse than that based on the minimized structures may be explained by the fact that all the evaluated systems are crystal structures, and many of them have even been used for the optimization of the MM/GBSA parameters.[41-43]

Therefore, the structural adjustment from the MD simulations may disturb the best positions of the ligands in the crystal structures. However, the MM/PBSA predictions based on the MD trajectories are indeed better than those based on the minimized structures (with the Pearson and Spearman coefficients of 0.491 and 0.561 compared with 0.412 and 0.500 when the inner dielectric constant was set to 4), indicating that MM/PBSA designed with a more physically rigorous model may be more favorable in the adjustment of the binding energy. Nevertheless, the overall accuracy of MM/PBSA based on the MD trajectories (r_p=0.491±0.003 and r_s=0.561±0.002) is still worse than that of MM/GBSA based on the MD trajectories (r_p=0.564±0.002 and r_s=0.591±0.002), which seems inconsistent with our previous work[51] as biased sampling was used in the evaluation (Some groups contain hundreds of instances, while most groups contain only one instance as shown below). However, the correlation and ranking scores (a criterion averaged all the r_p/r_s of the investigated systems on individual-fold-level, and here 29 fold families were used for the comparison as shown below, which may represent unbiased sampling) given by MM/PBSA for individual protein families are approximately equal or even a bit higher than those given by MM/GBSA (Table IV), suggesting that MM/PBSA can perform better on the individual-system level.[51] The details will be discussed below. It was found that eight systems were too large for the *pbsa* module in AMBER to solve the PB equation. For a fair comparison, the 8 systems were eliminated for the MM/GBSA calculations as well, thereby, as mentioned above, a total of 1864 systems were remained for the evaluation. The best predicted binding free energies (calculated by MM/GBSA method based on the minimized structures and 1 ns MD trajectories and a dielectric constant of 4) could be found in Supporting Information Table S1.

Indeed, even for the MM/GBSA predictions based on the minimized structures and the solute dielectric constant of 4, the Pearson correlation coefficient and Spearman ranking coefficient are only 0.579 and 0.602, respectively. Interestingly, a recent publication by Greenidge et al[52] as mentioned above showed that the MM/GBSA calculations based on a variable dielectric GB model (VSGB 2.0) could improve the Pearson coefficient to ~0.79 (r_p^2=0.63),[53] which is much higher than that

given by our study. However, when we evaluated the dataset used in the Greenidge's study, the MM/GBSA predictions based on the minimized structures and solute dielectric constant of 4 also gave comparable predictions, with the Pearson correlation coefficient and Spearman ranking coefficient up to 0.752 and 0.760, respectively (Figure 2). Greenidge et al. designed many rules to select the crystal structures used for method assessment, and therefore many structures were filtered out by the rules. However, in this study, we retained most structures in the PDBbind refined dataset (only the structures containing metal atoms have been removed). Therefore, our strategy may be more robust and comprehensive to reveal the actual prediction accuracies of MM/GBSA and MM/PBSA. Besides, it should be noted that, as shown in Figure 1, the predicted binding affinities by MM/GB(PB)SA are unphysically large (-120~-20 kcal/mol) compared with those derived from the experimental data (-16~-2 kcal/mol). This indicates that both MM/GBSA and MM/PBSA may be failed in reproducing the absolute binding free energy. Thereby, to some extent, it may regard the predicted binding affinities as MM/GBSA or MM/PBSA scores but not the true binding affinities.

Impact of ligand formal charges on the prediction accuracies of MM/GBSA and MM/PBSA

Ligand charge plays an important role in the binding of a ligand to its target. In this section, we evaluated the impact of the number of the ligand formal charges on the prediction accuracies of MM/GBSA and MM/PBSA. As shown in Figure 3, the overall accuracy becomes worse with the increase of the ligand formal charges, which means the methodologies (MM/GBSA and MM/PBSA) may fail in the predictions for the systems with high ligand charges. It can be found in Table II that the prediction accuracy of MM/GBSA, indicated by r_p and r_s, can rise to 0.621 and 0.641, respectively, when the number of ligand formal charges is 0 (neutral ligand). When the number of ligand formal charges is 1, the predictions become a bit worse (r_p and r_s are 0.578 and 0.618, respectively), but are still acceptable. However, the predictions become much worse (r_p=0.125~0.524, r_s=0.285~0.538) when the number of ligand

formal charges is more than 1. Greenidge's work has shown that the number of ligand formal charges does not have substantial impact on the prediction accuracy of MM/GBSA based on VSGB 2.0 that uses a variable dielectric constant ranged from 1 to 4. But if only these structures in the Greenidge's dataset were used in the evaluation, the r_p and r_s values of the charged ligands only slightly decrease to 0.723 and 0.730, compared with those of the neutral ligands (r_p=0.771±0.005 and r_s=0.778±0.005) (Figure 4). That is to say, for the Greenidge's dataset, our predictions given by MM/GBSA or MM/PBSA are also not quite sensitive to the number of ligand formal charges. However, according to the predictions based on the enlarged dataset used in this study, the impact of the ligand formal charges on the prediction accuracies of MM/GBSA and MM/PBSA becomes obviously. This may partly attribute to the unbalanced samples in some groups, such as the groups containing 5 and 6 formal charges only involve 10 and 13 samples, respectively, thereby lead to large uncertainties (Table II). However, even considering the upper limits of the uncertainties (using the upper r_p or r_s to give a comparison), the performance of MM/GBSA and MM/PBSA are still worse in the prediction of ligands with high formal charges (Figure 3).

The overall prediction accuracy of MM/PBSA is worse than that of MM/GBSA, whereas the predictions accuracy of MM/PBSA for the neutral and 1 charged ligands based on the MD trajectories are comparative to that of MM/GBSA based on the minimized structures. As shown in Table II, the MM/GBSA and MM/PBSA approaches can give more reliable predictions of the binding affinity for the ligands with the total formal charges of 0 and 1.

The prediction accuracies of MM/GBSA and MM/PBSA at the fold family level

A total of 1546 proteins were successfully mapped to 240 protein folds according to the SCOP database (version 1.75B, http://scop.berkeley.edu/), which hierarchically classifies protein architectures into several levels, such as *class*, *fold*, *superfamily*, *family*, etc., based on the structural features and sequence similarities of a diverse set of crystal structures.[73] It can be found in Figure 5 that the distribution of the protein

folds follows a Power-law-like behavior, where the number of the protein folds decays with the increase of their occurrence in the fold space. For two protein folds, namely b.47.1.2 and b.50.1.1, which take up only 0.8% of the investigated fold families, each is shared by more than 200 ligands, while for 123 protein folds (51.3%), each has just one ligand, meaning that much unbalanced samples are across the PDBbind dataset. If only considering one instance in each fold family (240 folds), decreased Pearson and Spearman coefficients will go across all the categories (Table III) compared with those in the corresponding overall accuracies (Table I). In fact, it may represent the true accuracies of the MM/GBSA and MM/PBSA methodologies which do not depend on the number of instances incorporated in a protein family. Thus, the methods (MM/GBSA and MM/PBSA) may be happened to work well on individual-fold-level due to the fact that the increased fold instances could indeed improve the prediction accuracies (Table I). To this end, in order to make a good evaluation of the prediction accuracies of MM/GBSA and MM/PBSA, we would better go back to the results based on individual protein folds.

According to Table IV, the proteins bounded with more than 9 ligands belonging to a same protein family take up ~60% of the investigated crystal structures (1109/1864). It can be found that the performance of MM/GBSA and MM/PBSA for many groups are much better than the highest overall accuracy (r_p=0.579±0.002 and r_s=0.602±0.002, Table I), for example, the family of b.47.1.2, which denotes the thrombin-like protein family and is the largest group of the dataset (226 individuals), has its r_p and r_s of 0.797 and 0.782, respectively. However, as shown in Figure 6, the second largest group with 220 complexes (b.50.1.1) performed much worse. Given the fact that the proteins in the family b.50.1.1 are HIV proteases, it is not surprising that the accurate prediction for this fold cannot be achieved. For example, Greenidge *et al.*[52] found that the ignorance of water-bridge had significant impact on the prediction of the binding free energy for the HIV proteases, and Lafont *et al.*[74] argued that the HIV protease is an "enthalpic and entropic compensated" system since the binding of drugs can seriously affect the motion of the flap of the HIV-1 protease. Therefore, it seems that the entropic contribution can significantly affect the binding

free energies of the ligands of the HIV-1 protease. Unfortunately, the expensive computational demand hindered us adding the entropic term to the predicted binding free energies. Moreover, the close distribution of the experimental binding free energies may also contribute to the low correlation for the b.50.1.1 family, where most drugs are crowded into the region of -14 to -10 kcal/mol (Figure 6D). However, the distribution of the ligands in b.47.1.2 is more balanced compared with that in b.50.1.1, with most of the ligands ranged from -12 to -5 kcal/mol (Figure 6C). If only the compounds located in the region of -14~-10 kcal/mol in the group b.47.1.2 were used in the predictions, the Pearson correlation r_p becomes only 0.3, which is much worse than that based on all compounds in the group b.47.1.2. For the third largest group d.144.1.7 that contains 118 individuals belonging to the tyrosine kinase family, the predictions are worse either (r_p and r_s = ~0.5), but still acceptable compared with the predictions for the group b.50.1.1 (Table IV). It is well known that the tyrosine kinase inhibitors can be roughly divided into two classes, Type I inhibitors and Type II inhibitors, which bind to the ATP-binding pocket and the allosteric pocket, respectively. However, as shown in Figure 7, both of the two classes of inhibitors can directly interact with the P-loop and/or A-loop region(s) (activation loop) of the tyrosine kinase that are flexible and associated with a substantial change of the conformational entropy during the binding of small molecules.[27, 36, 75, 76] Hence, the ignorance of entropy may be one reason for the low correlation coefficients for the tyrosine kinase family.

It has been mentioned above that the overall prediction accuracy of MM/PBSA is worse than that of MM/GBSA based on the currently available PDBbind dataset, but here at the fold family level, the correlation and ranking scores given by MM/PBSA are comparable to (or even slightly better than) those given by MM/GBSA (this is consistent with our previous study[51] and the case of one-protein-family/one-binding-ligand as discussed above), indicating that MM/PBSA is more sensitive to the investigated systems, and may be more suitable for the individual-target-level binding free energy ranking. Meanwhile, both MM/GBSA and MM/PBSA approaches can be used in virtual screening for

well-tested systems, such as the rescoring of the docking results for the groups of a.45.1.1, b.47.1.2, b.50.1.2, b.60.1.1, c.1.2.4, c.26.1.4, c.45.1.2, c.69.1.1, d.5.1.1, d.68.2.2, e.3.1.1, and e.8.1.4, which all have the Pearson and Spearman coefficients >0.6, as shown in Table IV. However, for a blind searching, such as reverse molecular docking, where many different drug targets were docked using a given set of small molecules, MM/GBSA will be more accurate based on the minimized structures and the dielectric constant of 4 (Table I). Moreover, as listed in Table IV, the correlation and ranking scores given by MM/PBSA based on the minimized structures is slightly better than those based on the 1 ns MD trajectories, implying that, rather than the overall accuracies of MM/PBSA (minimized and 1 ns trajectory results), it depends, whether to perform MD simulations to improve the prediction results, when an individual system is to be evaluated.

Conclusions

We have systemically investigated the overall prediction accuracies of MM/GBSA (GB^{OBC1}) and MM/PBSA (PB^{pbsa}) methodologies using more than 1800 ligand-receptor complexes. The results can be concluded as follows:

(1) Both the unbiased accuracies (the one-protein-family/one-binding-ligand case or the correlation/ranking score case) and the overall accuracies (based on the 1864 protein-ligand complexes), indicated by the Pearson correlation and Spearman ranking coefficients, reach the best when a dielectric constant of 4 was used in both MM/GBSA and MM/PBSA calculations. For the one-protein-family/one-binding-ligand case, the accuracies are similar between MM/GBSA and MM/PBSA in the minimized structures and the 1-ns MD trajectories. While for the overall case (1864 individuals), the MM/GSBA predictions based on the minimized structures are slightly better than those based on the 1 ns MD trajectories, and the MM/PBSA predictions based on the 1 ns MD trajectories have better overall accuracy than those based on the minimized structures but are still worse than the MM/GBSA predictions. Therefore, considering the currently used PDBbind dataset,

MM/GSBA can be used in most cases, such as reverse molecular docking.

(2) The accuracies of both MM/GBSA and MM/PBSA predictions decrease with the increase of the number of ligand formal charges, implying that the predictions for low charged or neutral ligands are more reliable.

(3) At the fold family level (another kind of unbiased sampling case), the ranking and correlation scores given by MM/PBSA are comparable to those given by MM/GBSA, indicating that MM/PBSA is more sensitive to the investigated systems than MM/GBSA, and may be more suitable for the individual-target-level prediction. Therefore, the structural based classification is needed to distinguish which groups can be reliably predicted by which approach (MM/PBSA or MM/GBSA).

Acknowledgment

This study was supported by the National Science Foundation of China (21173156), the National Basic Research Program of China (973 program, 2012CB932600), and the Priority Academic Program Development of Jiangsu Higher Education Institutions (PAPD).

Supporting information

Table S1. Crystal structures and predicted binding free energies in this study.

References

1 H. Gohlke, C. Kiel and D. A. Case, *J. Mol. Biol.* , 2003, **330**, 891-914.
2 H. Gohlke and G. Klebe, *Angew. Chem. Int. Edit.*, 2002, **41**, 2644-2676.
3 T. Hou, Z. Xu, W. Zhang, W. A. McLaughlin, D. A. Case, Y. Xu and W. Wang, *Mol. Cell Proteomics.*, 2009, **8**, 639-649.
4 T. Hou and W. Zhang, *J. Mol. Biol.*, 2008, **376**, 1201-1214.
5 T. Hou, W. Zhang, J. Wang and W. Wang, *Proteins: Struct., Funct., Bioinf.*, 2009, **74**, 837-846.
6 T. J. Hou, S. L. Guo and X. J. Xu, *J. Phys. Chem. B.*, 2002, **106**, 5527-5535.
7 T. J. Hou, N. Li, Y. Y. Li and W. Wang, *J. Proteome Res.*, 2012, **11**, 2982-2995.
8 T. J. Hou, Y. Y. Li and W. Wang, *Bioinformatics*, 2011, **27**, 1814-1821.
9 T. J. Hou, L. L. Zhu, L. R. Chen and X. J. Xu, *J. Chem. Inf. Comput. Sci.*, 2003, **43**, 273-287.
10 S. Huo, I. Massova and P. A. Kollman, *J. Comput. Chem.*, 2002, **23**, 15-27.

11 S. Huo, J. Wang, P. Cieplak, P. A. Kollman and I. D. Kuntz, *J. Comput. Chem.*, 2002, **45**, 1412-1419.

12 B. Kuhn and P. A. Kollman, *J. Med. Chem.*, 2000, **43**, 3786-3791.

13 H. Liu and X. Yao, *Mol. Pharmaceut.*, 2009, **7**, 75-85.

14 E. Muzzioli, A. Del Rio and G. Rastelli, *Chem. Biol. Drug Des.*, 2011, **78**, 252-259.

15 C. S. Page and P. A. Bates, *J. Comput. Chem.*, 2006, **27**, 1990-2007.

16 J. Wang, P. Morin, W. Wang and P. A. Kollman, *J. Am. Chem. Soc.*, 2001, **123**, 5221-5230.

17 W. Wang, W. A. Lim, A. Jakalian, J. Wang, J. Wang, R. Luo, C. I. Bayly and P. A. Kollman, *J. Am. Chem. Soc.*, 2001, **123**, 3986-3994.

18 Z. Xu, T. Hou, N. Li, Y. Xu and W. Wang, *Mol. Cell. Proteomics*, 2012, **11**, O111.010389.

19 Y. Yang, J. Qin, H. Liu and X. Yao, *J. Chem. Inf. Model.*, 2011, **51**, 680-692.

20 Y. Yang, H. Liu and X. Yao, *Mol. Biosystems*, 2012, **8**, 2106-2118.

21 W. Xue, X. Jin, L. Ning, M. Wang, H. Liu and X. Yao, *J. Chem. Inf. Model.*, 2012, **53**, 210-222.

22 S. Genheden, I. Nilsson and U. Ryde, *J. Chem. Inf. Model.*, 2011, **51**, 947-958.

23 P. Mikulskis, S. Genheden, P. Rydberg, L. Sandberg, L. Olsen and U. Ryde, *J. Comput.-aided Mol. Des.*, 2012, **26**, 527-541.

24 S. Genheden and U. Ryde, *J. Chem. Theo. Comput.* , 2011, **7**, 3768-3778.

25 Q. Xue, J.-L. Zhang, Q.-C. Zheng, Y.-L. Cui, L. Chen, W.-T. Chu and H.-X. Zhang, *Langmuir*, 2013, **29**, 11135-11144.

26 Y.-L. Cui, Q.-C. Zheng, J.-L. Zhang, Q. Xue, Y. Wang and H.-X. Zhang, *J. Chem. Inf. Model.*, 2013.

27 L. Chen, J.-L. Zhang, L.-Y. Yu, Q.-C. Zheng, W.-T. Chu, Q. Xue, H.-X. Zhang and C.-C. Sun, *J. Phys. Chem. B.*, 2012, **116**, 12415-12425.

28 H. Gohlke and G. Klebe, *Angew. Chem. Int. Ed. Engl.*, 2002, **41**, 2644-2676.

29 D. L. Beveridge and F. DiCapua, *Annu. Rev. Biophys. Biophys. Chem.*, 1989, **18**, 431-492.

30 W. L. Jorgensen and L. L. Thomas, *J. Chem. Theory Comput.*, 2008, **4**, 869-876.

31 S. Zhu, S. M. Travis and A. H. Elcock, *J. Chem. Theory Comput.*, 2013.

32 S. Jo, W. Jiang, H. S. Lee, B. Roux and W. Im, *J. Chem. Inf. Model.*, 2013, **53**, 267-277.

33 D. L. Mobley, J. D. Chodera and K. A. Dill, *J. Chem. Phys.*, 2006, **125**, 084902.

34 C. Gao, M.-S. Park and H. A. Stern, *Biophys. J.*, 2010, **98**, 901-910.

35 T. Hou and R. Yu, *J. Med. Chem.*, 2007, **50**, 1177-1188.

36 H. Sun, Y. Li, D. Li and T. Hou, *J. Chem. Inf. Model.*, 2013, **53**, 2376-2389.

37 L. Xu, Y. Li, S. Zhou and T. Hou, *Mol. BioSyst.*, 2012, **8**, 2260-2273.

38 W. Xue, D. Pan, Y. Yang, H. Liu and X. Yao, *Antiviral Res.*, 2012, **93**, 126-137.

39 J. Zhang, T. Hou, W. Wang and J. S. Liu, *Proc. Natl. Acad. Sci. USA*, 2010, **107**, 1321-1326.

40 H.-Y. Sun, F.-Q. Ji, L.-Y. Fu, Z.-Y. Wang and H.-Y. Zhang, *J. Chem. Inf. Model.*, 2013, **53**, 3343-3351.

41 A. Onufriev, D. Bashford and D. A. Case, *Proteins: Struct., Funct., Bioinf.*, 2004, **55**, 383-394.

42 G. D. Hawkins, C. J. Cramer and D. G. Truhlar, *Chem. Phys. Lett.*, 1995, **246**, 122-129.

43 G. D. Hawkins, C. J. Cramer and D. G. Truhlar, *J. Phys. Chem.*, 1996, **100**, 19824-19839.

44 V. Tsui and D. A. Case, *Biopolymers*, 2000, **56**, 275-291.

45 C. P. Kelly, C. J. Cramer and D. G. Truhlar, *J. Phys. Chem. B.*, 2006, **110**, 16066-16081.

46 T. Hou, J. Wang, Y. Li and W. Wang, *J. Chem. Inf. Model.*, 2011, **51**, 69-82.

47 S. Genheden, O. Kuhn, P. Mikulskis, D. Hoffmann and U. Ryde, *J. Chem. Inf. Model.*, 2012, **52**,

2079-2088.
48 T. Hou, J. Wang, Y. Li and W. Wang, *J. Comput. Chem.*, 2011, **32**, 866-877.
49 I. Maffucci and A. Contini, *J. Chem. Theory Comput.*, 2013, **9**, 2706-2717.
50 A. Weis, K. Katebzadeh, P. Söderhjelm, I. Nilsson and U. Ryde, *J. Med. Chem.*, 2006, **49**, 6596-6606.
51 L. Xu, H. Sun, Y. Li, J. Wang and T. Hou, *J. Phys. Chem. B.*, 2013, **117**, 8408-8421.
52 P. A. Greenidge, C. Kramer, J.-C. Mozziconacci and R. M. Wolf, *J. Chem. Inf. Model.*, 2013, **53**, 201-209.
53 J. Li, R. Abel, K. Zhu, Y. Cao, S. Zhao and R. A. Friesner, *Proteins: Struct., Funct., Bioinf.*, 2011, **79**, 2794-2812.
54 R. Wang, X. Fang, Y. Lu, C.-Y. Yang and S. Wang, *J. Med. Chem.*, 2005, **48**, 4111-4119.
55 R. Wang, X. Fang, Y. Lu and S. Wang, *J. Med. Chem.*, 2004, **47**, 2977-2980.
56 T. Cheng, X. Li, Y. Li, Z. Liu and R. Wang, *J. Chem. Inf. Model.*, 2009, **49**, 1079-1093.
57 C. Kramer, T. Kalliokoski, P. Gedeck and A. Vulpetti, *J. Med. Chem.*, 2012, **55**, 5165-5173.
58 J. Wang, W. Wang, P. A. Kollman and D. A. Case, *J. Mol. Graph. Model.*, 2006, **25**, 247-260.
59 A. Jakalian, D. B. Jack and C. I. Bayly, *J. Comput. Chem.*, 2002, **23**, 1623-1641.
60 R. C. Walker, M. F. Crowley and D. A. Case, *J. Comput. Chem.*, 2008, **29**, 1019-1031.
61 Y. Duan, C. Wu, S. Chowdhury, M. C. Lee, G. Xiong, W. Zhang, R. Yang, P. Cieplak, R. Luo and T. Lee, *J. Comput. Chem.*, 2003, **24**, 1999-2012.
62 J. Wang, R. M. Wolf, J. W. Caldwell, P. A. Kollman and D. A. Case, *J. Comput. Chem.*, 2004, **25**, 1157-1174.
63 W. L. Jorgensen, J. Chandrasekhar, J. D. Madura, R. W. Impey and M. L. Klein, *J. Chem. Phys.*, 1983, **79**, 926-935.
64 T. Darden, D. York and L. Pedersen, *J. Chem. Phys.*, 1993, **98**, 10089-10092.
65 J. P. Ryckaert, G. Ciccotti and H. J. C. Berendsen, *J. Comput. Phys.*, 1977, **23**, 327-341.
66 W. Rocchia, E. Alexov and B. Honig, *J. Phys. Chem. B.*, 2001, **105**, 6507-6514.
67 Q. Lu and R. Luo, *J. Chem. Phys.*, 2003, **119**, 11035-11048.
68 E. Muzzioli, A. Del Rio and G. Rastelli, *Chem. Biol. Drug Des.*, 2011, **78**, 252-259.
69 J. Weiser, P. S. Shenkin and W. C. Still, *J. Comput. Chem.*, 1999, **20**, 217-230.
70 J. D. Thompson, T. J. Gibson, F. Plewniak, F. Jeanmougin and D. G. Higgins, *Nucleic Acids Res.*, 1997, **25**, 4876-4882.
71 A. G. Murzin, S. E. Brenner, T. Hubbard and C. Chothia, *J. Mol. Biol.*, 1995, **247**, 536-540.
72 J. M. Chandonia, G. Hon, N. S. Walker, L. L. Conte, P. Koehl, M. Levitt and S. E. Brenner, *Nucleic. Acids. Res.*, 2004, **32**, D189-D192.
73 J.-M. Chandonia and S. E. Brenner, *Science*, 2006, **311**, 347-351.
74 V. Lafont, A. A. Armstrong, H. Ohtaka, Y. Kiso, L. Mario Amzel and E. Freire, *Chem. Biol. Drug Des.*, 2007, **69**, 413-422.
75 S. Betzi, R. Alam, M. Martin, D. J. Lubbers, H. Han, S. R. Jakkaraj, G. I. Georg and E. Schonbrunn, *ACS Chem. Biol.*, 2011, **6**, 492-501.
76 J. J. Cui, M. Tran-Dubé, H. Shen, M. Nambu, P. P. Kung, M. Pairish, L. Jia, J. Meng, L. Funk and I. Botrous, *J. Med. Chem.*, 2011, **54**, 6342-6363.

Legend of the Figures

Figure 1. Overall distribution of the 1864 systems used in this study. The minimized structures and the interior dielectric constant of 4 were used for the Pearson correlation coefficient calculation.

Figure 2. Pearson correlation for the Greenidge's dataset. The minimized structures and the interior dielectric constant of 4 were used to give a comparison. Due to the different protocol and the different version of PDBbind we used, only 814 PDBbind ID were mapped to the Greenidge's dataset (855). The Spearman ranking coefficient (r_s) of 0.760 is a bit higher than the Pearson correlation coefficient (r_p) of 0.752.

Figure 3. Change of the Pearson correlation coefficients (A) and Spearman ranking coefficients (B) with the number of ligand form charges predicted by various simulation protocols.

Figure 4. Pearson correlation coefficient and Spearman ranking coefficient for the neutral (A) and charged (B) ligands using the Greenidge's dataset based on the MM/GBSA calculations and inner dielectric constant of 4.

Figure 5. Distribution of the protein folds based on the *family* level SCOP index, where a Power-law like behavior was observed. The number of the protein folds (*N*) decays with the increase of their occurrence in the fold space (*S*).

Figure 6. Performance of the groups b.47.1.2 (A) and b.50.1.1 (B), and their corresponding distributions of the ligands (C and D) based on the MM/GBSA calculations and interior dielectric constant of 4. It can be found that the distribution of ligands in the group of b.50.1.1 is more unbalance than that of b.47.1.2.

Figure 7. A-loop and P-loop (yellow) in (A) ALK tyrosine kinase and (B) CDK tyrosine kinase. It can be found that the Type I inhibitor (A, orange) tightly interacts

with the P-loop region of ALK kinase, and the type II inhibitor (B, orange) can interact with not only P-loop, but also the A-loop region of CDK kinase, which are both involved in large conformational change when binding to the inhibitors.

Table I. Overall prediction accuracies of MM/GBSA and MM/PBSA based on various simulation protocols (a total of 1864 systems were used for the evaluation).

MM/GBSA			MM/PBSA		
Classification[a]	r_p[b]	r_s[c]	Classification	r_p[b]	r_s[c]
GB-1ns-1	0.353±0.002[d]	0.437±0.002	PB-1ns-1	0.071±0.002	0.198±0.003
GB-1ns-2	0.521±0.002	0.563±0.002	PB-1ns-2	0.306±0.004	0.480±0.002
GB-1ns-4	0.564±0.002	0.591±0.002	PB-1ns-4	0.491±0.003	0.561±0.002
GB-min-1	0.352±0.002	0.416±0.003	PB-min-1	-0.043±0.002	-0.041±0.003
GB-min-2	0.535±0.002	0.567±0.002	PB-min-2	0.152±0.002	0.248±0.003
GB-min-4	0.579±0.002	0.602±0.002	PB-min-4	0.412±0.003	0.500±0.002

[a]The classification is named by different simulation protocols, *i.e.* GB-1ns-1, where GB or PB denotes for MM/GBSA or MM/PBSA, -1 ns or -min means that the calculations were based on the 1 ns simulation trajectories or the minimized structures, and -1, -2, or -4 represents the interior dielectric constant of 1, 2, or 4 of for the GB or PB calculations; [b]r_p represents Pearson correlation coefficient; [c]r_s represents Spearman ranking coefficient; [d]The standard error was estimated by randomly sampling 80% of the tested dataset with 100 times.

Table II. Overall prediction accuracies of MM/GBSA and MM/PBSA for the datasets with different numbers of ligand formal charges (the interior dielectric constant of 4 was used)

Charge	Coefficient	GB-1ns	GB-min	PB-1ns	PB-min	Total
0	r_p	0.608±0.003[a]	0.621±0.003	0.594±0.003	0.551±0.003	780
	r_s	0.633±0.002	0.641±0.003	0.631±0.002	0.589±0.003	
1	r_p	0.564±0.003	0.578±0.003	0.569±0.003	0.537±0.003	663
	r_s	0.600±0.003	0.618±0.003	0.596±0.003	0.551±0.003	
2	r_p	0.452±0.005	0.471±0.005	0.409±0.005	0.328±0.006	286
	r_s	0.516±0.005	0.538±0.005	0.500±0.005	0.428±0.006	
3	r_p	0.567±0.010	0.524±0.012	0.471±0.012	0.319±0.011	82
	r_s	0.560±0.010	0.525±0.012	0.488±0.012	0.331±0.011	
4	r_p	0.434±0.031	0.367±0.035	0.421±0.029	0.341±0.025	30
	r_s	0.422±0.040	0.330±0.040	0.504±0.026	0.472±0.021	
5	r_p	0.094±0.157	0.125±0.142	0.061±0.093	0.165±0.067	10
	r_s	0.285±0.125	0.285±0.101	0.236±0.124	0.309±0.108	
6	r_p	0.343±0.079	0.417±0.098	0.136±0.074	0.199±0.068	13
	r_s	0.454±0.073	0.459±0.102	0.330±0.099	0.399±0.077	

[a]The standard error was estimated by randomly sampling 80% of the tested dataset with the repeat times of the *Total*, namely 780, 663, 286, 82, 30, 10, and 13 times for each group.

Table III. Unbiased prediction accuracies of MM/GBSA and MM/PBSA with one instance in the 240 fold families.

Dielectric constant	Coefficient	GB-1ns	GB-min	PB-1ns	PB-min
1	r_p	0.298±0.007[a]	0.298±0.008	0.179±0.010	0.195±0.007
	r_s	0.321±0.006	0.315±0.008	0.310±0.006	0.287±0.006
2	r_p	0.388±0.006	0.393±0.007	0.283±0.009	0.300±0.008
	r_s	0.407±0.006	0.405±0.006	0.401±0.006	0.399±0.006
4	r_p	0.406±0.005	0.408±0.006	0.371±0.007	0.388±0.006
	r_s	0.418±0.006	0.395±0.006	0.427±0.007	0.433±0.005

[a]The standard error was estimated by randomly selecting one instance from the fold families containing many instances (> 1) with 100 repeats.

Table IV. Overall prediction accuracies of MM/GBSA and MM/PBSA for the protein fold families with more than 9 ligands. The highest Pearson and Spearman coefficients and the corresponding solute dielectric constant ($\varepsilon_{GB}/\varepsilon_{PB}$) were listed.

SCOP ID	Dielectric constant	Correlation coefficient	GB-1ns	GB-min	PB-1ns	PB-min	Total
a.123.1.1	1[a]/4[b]	r_p	0.489±0.021[f]	0.540±0.024	0.426±0.023	0.495±0.022	48
		r_s	0.292±0.024	0.350±0.025	0.206±0.023	0.259±0.021	
a.133.1.2	1[c]	r_p	0.120±0.134	0.124±0.106	0.096±0.143	0.019±0.172	11
		r_s	0.236±0.126	0.282±0.120	0.010±0.167	0.009±0.164	
a.45.1.1	4	r_p	0.676±0.067	0.706±0.024	0.728±0.108	0.708±0.055	11
		r_s	0.683±0.086	0.706±0.052	0.761±0.122	0.797±0.037	
b.1.1.1	4/1	r_p	0.059±0.031	0.052±0.032	0.201±0.024	0.164±0.033	33
		r_s	0.084±0.037	0.095±0.037	0.275±0.032	0.281±0.033	
b.3.4.1	1	r_p	0.534±0.091	0.471±0.055	0.355±0.059	0.267±0.044	10
		r_s	0.590±0.061	0.596±0.077	0.432±0.050	0.432±0.046	
b.47.1.2	4	r_p	0.797±0.003	0.796±0.003	0.799±0.002	0.801±0.003	226
		r_s	0.782±0.003	0.784±0.003	0.780±0.003	0.787±0.003	
b.50.1.1	4	r_p	0.129±0.012	0.165±0.010	0.063±0.011	0.096±0.011	220
		r_s	0.070±0.009	0.100±0.009	-0.002±0.009	0.015±0.008	
b.50.1.2	4	r_p	0.693±0.019	0.761±0.013	0.678±0.016	0.700±0.014	44
		r_s	0.661±0.025	0.700±0.018	0.657±0.021	0.701±0.017	
b.60.1.1	1/2	r_p	0.813±0.012	0.726±0.022	0.831±0.009	0.778±0.015	20
		r_s	0.841±0.009	0.845±0.014	0.873±0.018	0.834±0.016	
b.60.1.2	4	r_p	0.368±0.086	0.325±0.060	0.388±0.058	0.257±0.043	15
		r_s	0.322±0.097	0.243±0.073	0.356±0.074	0.111±0.062	
b.61.1.1	1	r_p	0.070±0.050	0.211±0.108	0.213±0.067	0.534±0.077	13
		r_s	0.148±0.083	0.242±0.105	0.264±0.096	0.670±0.078	
c.1.1.1	1	r_p	0.373±0.115	0.022±0.125	0.329±0.161	0.071±0.115	11
		r_s	0.218±0.117	0.018±0.127	0.100±0.169	0.218±0.154	
c.1.2.4	1/2	r_p	0.897±0.201	0.976±0.139	0.901±0.230	0.980±0.047	9
		r_s	0.333±0.173	0.804±0.113	0.473±0.216	0.770±0.061	
c.1.8.3	1	r_p	0.237±0.080	0.329±0.048	0.046±0.074	0.563±0.031	17
		r_s	0.042±0.083	0.128±0.065	0.142±0.077	0.733±0.048	
c.1.8.4	4	r_p	0.217±0.060	0.273±0.067	-0.021±0.052	-0.016±0.051	21
		r_s	0.008±0.052	0.160±0.079	-0.014±0.059	-0.100±0.054	
c.26.1.4	4	r_p	0.619±0.040	0.664±0.045	0.658±0.068	0.695±0.035	16
		r_s	0.540±0.055	0.550±0.075	0.624±0.066	0.696±0.058	
c.45.1.2	4	r_p	0.649±0.018	0.708±0.016	0.688±0.019	0.751±0.014	32
		r_s	0.677±0.018	0.712±0.018	0.678±0.020	0.752±0.015	
c.56.2.1	4	r_p	0.525±0.031	0.495±0.026	0.508±0.031	0.469±0.042	24
		r_s	0.499±0.040	0.408±0.041	0.449±0.044	0.312±0.054	
c.69.1.1	4	r_p	0.763±0.050	0.792±0.059	0.705±0.052	0.729±0.121	13

		r_s	0.654±0.071	0.588±0.102	0.632±0.056	0.560±0.124	
c.87.1.4	1	r_p	0.062±0.093	0.300±0.081	-0.365±0.125	0.479±0.043	19
		r_s	0.223±0.065	0.316±0.067	0.029±0.109	0.498±0.047	
d.93.1.1	4	r_p	0.488±0.070	0.621±0.111	0.372±0.132	0.583±0.096	9
		r_s	0.410±0.121	0.494±0.144	0.427±0.121	0.544±0.106	
c.94.1.1	1/4	r_p	0.277±0.018	0.342±0.015	0.193±0.020	0.253±0.020	58
		r_s	0.278±0.017	0.329±0.016	0.213±0.017	0.236±0.020	
d.117.1.1	4	r_p	0.547±0.153	0.713±0.074	0.476±0.081	0.579±0.098	12
		r_s	0.175±0.142	0.378±0.098	0.161±0.098	0.315±0.098	
d.122.1.1	1/4	r_p	0.601±0.050	0.532±0.064	0.336±0.036	0.346±0.065	21
		r_s	0.336±0.067	0.279±0.060	0.056±0.040	0.144±0.069	
d.144.1.7	4/2	r_p	0.499±0.006	0.497±0.007	0.524±0.006	0.498±0.008	118
		r_s	0.555±0.007	0.533±0.008	0.558±0.007	0.530±0.009	
d.5.1.1	4	r_p	0.571±0.040	0.628±0.028	0.658±0.026	0.712±0.026	35
		r_s	0.407±0.020	0.514±0.024	0.554±0.024	0.667±0.018	
d.68.2.2	4	r_p	0.824±0.028	0.778±0.028	0.801±0.051	0.806±0.035	10
		r_s	0.818±0.028	0.806±0.036	0.794±0.052	0.794±0.056	
e.3.1.1	4	r_p	0.714±0.025	0.698±0.018	0.699±0.047	0.681±0.027	21
		r_s	0.710±0.028	0.647±0.029	0.636±0.058	0.592±0.027	
e.8.1.4	4	r_p	0.702±0.037	0.706±0.044	0.684±0.051	0.683±0.057	12
		r_s	0.790±0.048	0.811±0.052	0.783±0.047	0.783±0.062	
Correlation score (r_p score)[d]			0.494±0.047[g]	0.516±0.047	0.447±0.057	0.506±0.050	1109
Ranking score (r_s score)[e]			0.427±0.048	0.463±0.047	0.411±0.052	0.481±0.052	

[a,b]The corresponding interior dielectric constants for achieving the best [a]MM/GBSA and [b]MM/PBSA predictions; [c]A same interior dielectric constant was found in best MM/GBSA and MM/PBSA predictions; [d,e]The [d]correlation score or [e]ranking score is the average of the summation of the r_p or r_s for the above fold families, and they have been proven to be effective in distinguishing a series of similar results [51]. [f]The standard error was estimated by randomly sampling 80% of the tested dataset with the repeat times of the *Total*. [g]The standard error was calculated based on the 29 groups above.

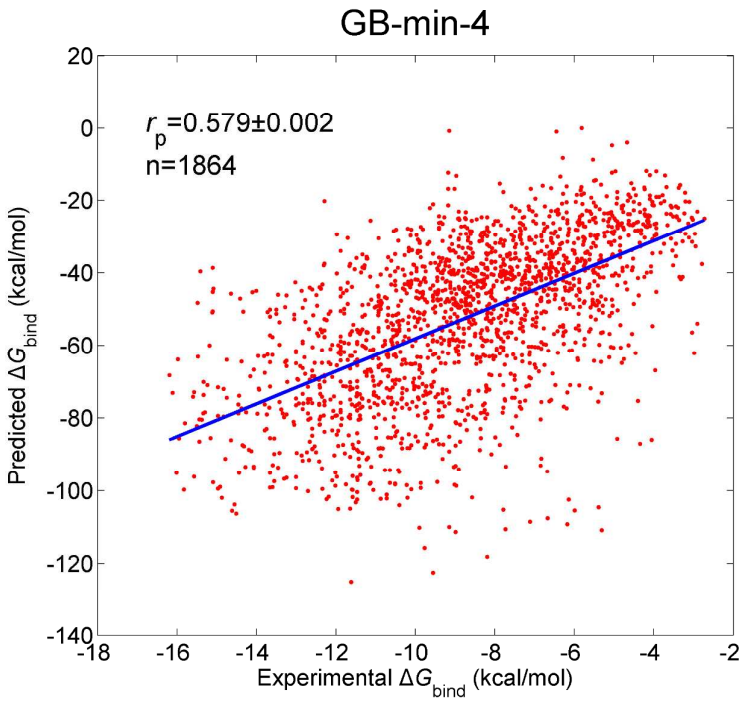

Figure 1

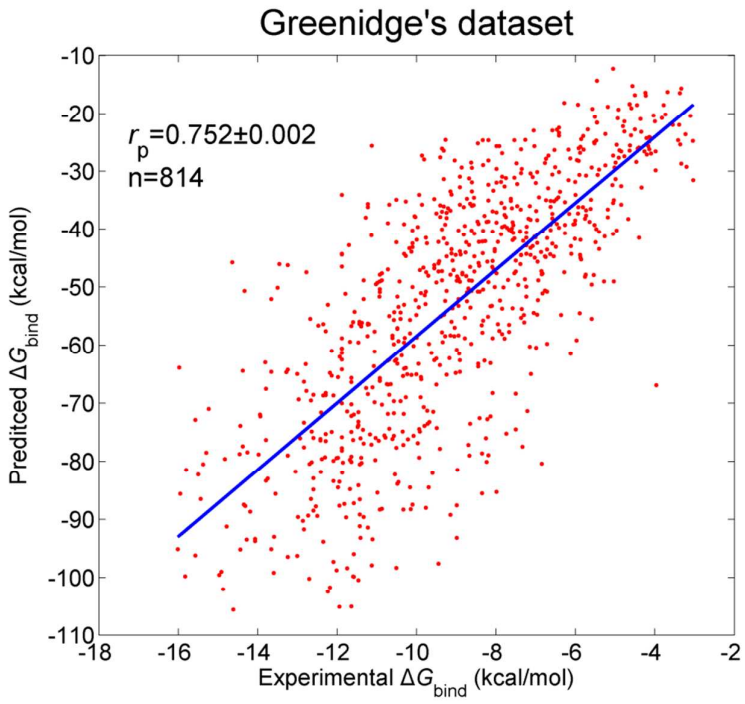

Figure 2

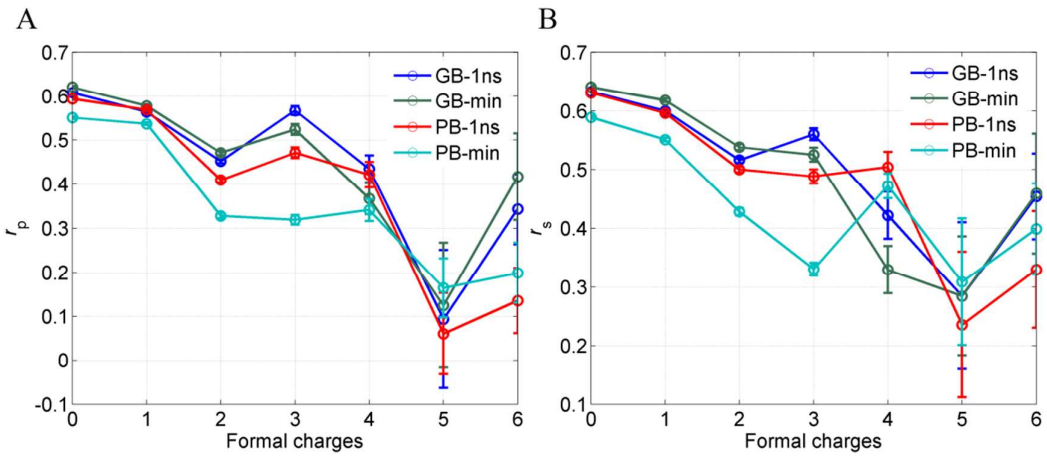

Figure 3

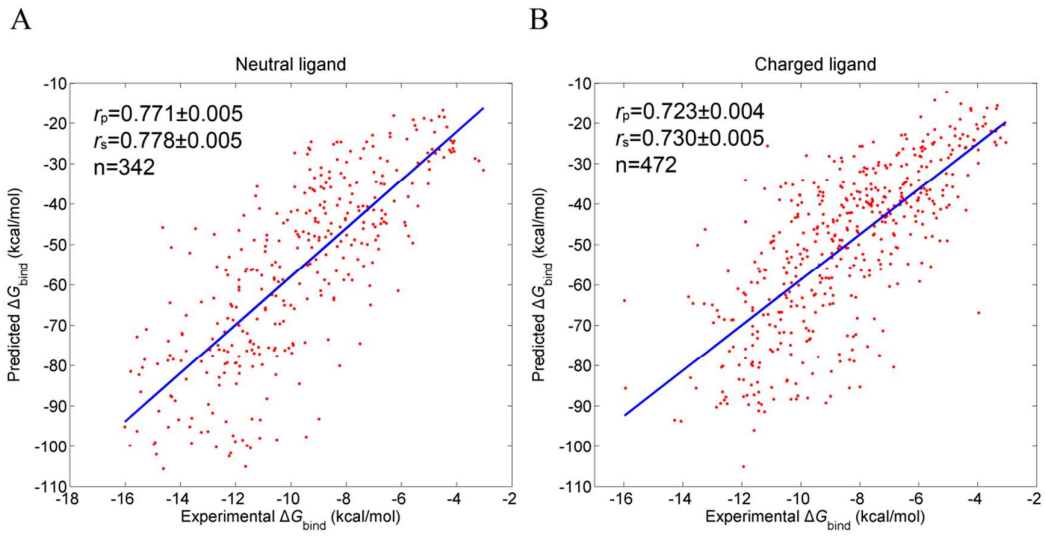

Figure 4

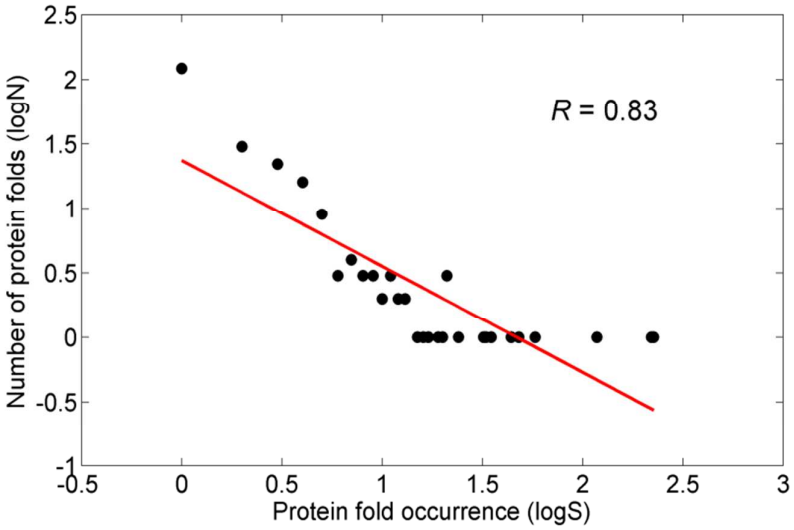

Figure 5

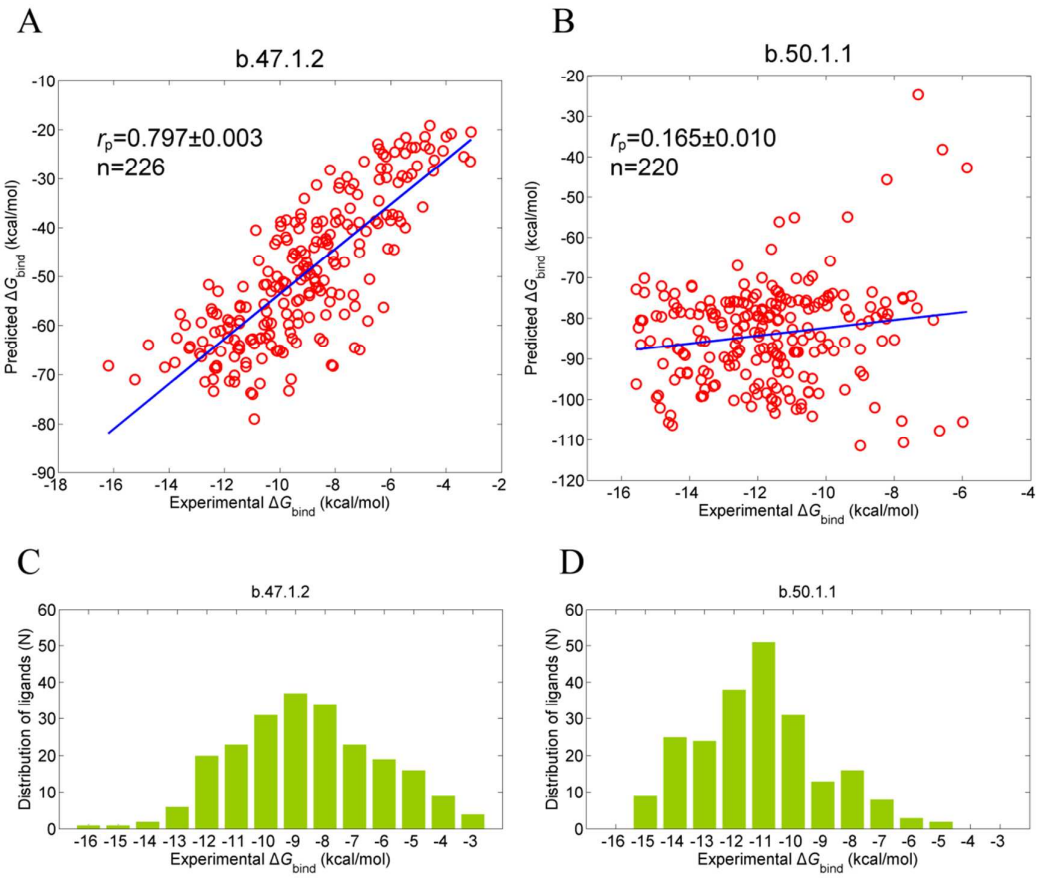

Figure 6

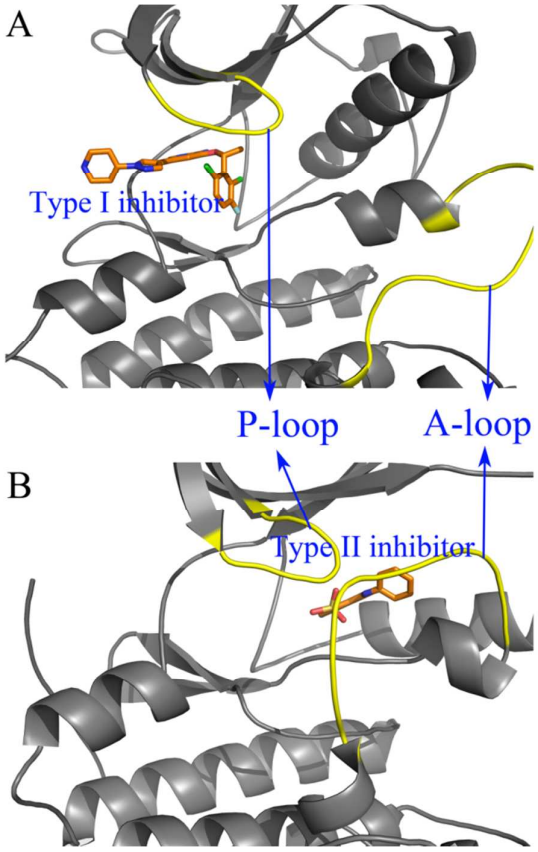

Figure 7

For Table of Contents Use Only

Formal Charges

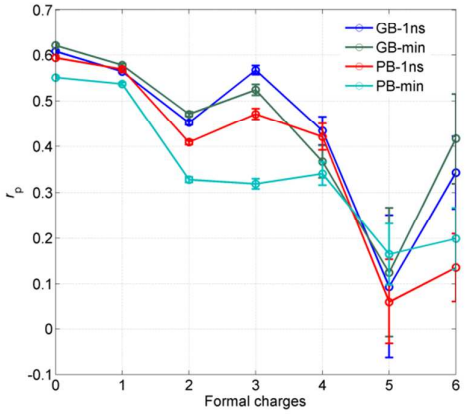

Fold Family